Mass and Heat Transfer in Crushed Oil Shale

James F. Carley and Linda L. Ott
Lawrence Livermore National Laboratory, Livermore, CA 94550

Jeanne L. Swecker
Corning, Inc., Telecommunication Products Div., Wilmington, NC 28405

Studies of heat and mass transfer in packed beds, which disagree substantially in their findings, have nearly all been done with beds of regular particles of uniform size, whereas oil-shale retorting involves particles of diverse irregular shapes and sizes. We, in 349 runs, measured mass-transfer rates from naphthalene particles buried in packed beds by passing through air at room temperature. An exact analogy between convection of heat and mass makes it possible to infer heat-transfer coefficients from measured mass-transfer coefficients and fluid properties. Some beds consisted of spheres, naphthalene and inert, of the same, contrasting or distributed sizes. In some runs, naphthalene spheres were buried in beds of crushed shale, some in narrow screen ranges and others with a wide size range. In others, naphthalene lozenges of different shapes were buried in beds of crushed shale in various bed axis orientations. This technique permits calculation of the mass-transfer coefficient for each active particle in the bed rather than, as in most past studies, for the bed as a whole.

The data are analyzed by the traditional correlation of Colburn j_D vs. Reynolds number and by multiple regression of the mass-transfer coefficient on air rate, sizes of active and inert particles, void fraction, and temperature. Principal findings are: local Reynolds number should be based on the active-particle size, not the average for the whole bed; differences between shallow and deep beds are not appreciable; mass transfer is 26% faster for spheres and lozenges buried in shale than in all-sphere beds; orientation of lozenges in shale beds has little or no effect on mass-transfer rate; and for mass or heat transfer in shale beds, $\log(j \cdot \epsilon) = -0.0747 - 0.6344 \log N_{Re} + 0.0592 \log^2 N_{Re}$.

Introduction

Convection of heat and mass between gases and the particles of packed beds are important processes in recovery of oil from oil shale. A preliminary survey of the literature turned up several different ways of correlating such information and also revealed substantial disagreement among the results of different investigators. For example, see Bird et al. (1960, p. 411) and the survey report by Kunii and Suzuki (1967) or the plot reproduced from that report in the text of Kunii and Levenspiel (1967). The most comprehensive survey was that of Whitaker (1972), who collected and presented the results of seven publications by Hougen, Thodos, and coworkers on a bilogarithmic plot of $N_{Nu}/N_{Pr}^{1/3}$ vs. Re (each specially defined) on which the latter had fitted the equation

$$N_{Nu} N_{Pr}^{-1/3} = 0.60\, N_{Re}^{-0.60}. \tag{1}$$

The point scatter around this line (and the two-term, weakly curved equation later fitted by Whitaker) was about a factor of 2 above and below. We found, too, that with just a few exceptions, all the studies had been made with beds composed of smooth, regular particles of a single size such as glass marbles or Raschig rings. Another characteristic of these

Correspondence concerning this article should be addressed to J. F. Carley, 579 Ruby Rd., Livermore, CA 94550.

studies was that, by the nature of the measurements, the transfer coefficients—heat or mass—were averaged over the entire bed, so little was learned about local rates within the bed. In our detailed computer modeling of oil-shale retorting, we wished to treat local regions—even individual pieces of oil shale—within the retort according to the conditions prevailing there and we expected to have to deal with a range of particle sizes at all points. For all these reasons we decided to make a new investigation of transfer in packed beds, with particular attention to crushed oil shale.

Professor H. Y. Sohn of the University of Utah suggested that, because local measurements of heat-transfer coefficients within packed beds were very difficult to make, we could measure mass-transfer coefficients instead, then use the exact analogy between the two processes (Bird et al., 1960, p. 646) to infer heat-transfer coefficients from the mass-transfer coefficients. By planting particles of naphthalene within the bed and observing their loss of weight as air was passed through the bed at a steady rate, the rate of mass transfer and the coefficient could be calculated for each particle.

Experimental Plan

Naphthalene was chosen for this work, as it has been for earlier studies, because of its convenient combination of properties: (1) it is readily available in pure crystals; (2) it is solid at room temperature but melts at 80°C and can be cast into various shapes; (3) its vapor pressure at room temperature is low, about 9 Pa, but high enough so that in a few hours of exposure to moving air, there is an accurately measurable loss of mass from particles weighing a gram or more; and (4) its vapor pressure and diffusivity are known. (But not as accurately known as was earlier believed, a point we shall address later.) Naphthalene vapor is toxic, so melting and casting specimens and the mass-transfer work must be carried on in a competent hood. We used simple aluminum molds to cast spheres of sizes ranging from 1.27 to 5 cm (0.5 to 2 in.) and later, other molds to cast three rectangular shapes. Reporting about these castings is much easier than producing them free of defects, but we eventually developed successful techniques.

The plan was to proceed in four stages, as follows:

In Stage 1, experiments would be made with naphthalene spheres buried in beds of unisize inert balls, the idea being to confirm earlier work made in similar beds and to define the roles of the active- and inert-sphere sizes in the transfer process. By placing two or more closely identical naphthalene balls in a single bed of uniform inert spheres, we would also establish the point-to-point variation in the rate of naphthalene evaporation that could be expected because of local differences in bed geometry—even with spheres—and air velocity around the balls.

In Stage 2, naphthalene spheres would be immersed in beds consisting of balls of mixed sizes.

In Stage 3, spheres would be placed within beds of crushed shale having narrow and broad size distributions.

In Stage 4, we would immerse, in beds of crushed shale, naphthalene particles shaped more nearly like shale particles, yet regular enough to have accurately calculable surface areas. For this duty we chose rectangular parallelopipeds

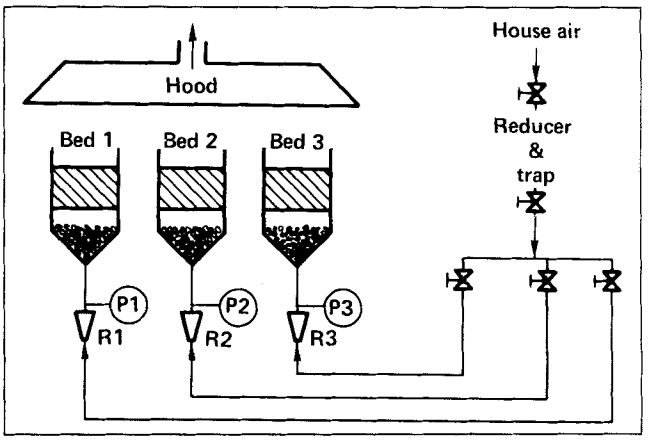

Figure 1. Experimental setup.

("rectapipeds" or "lozenges") of three rather different aspect ratios, and would try several orientations of each with respect to the bed axis.

Experimental Details

Figure 1 is a schematic diagram of the experimental equipment, which was set up in triplicate to permit simultaneously carrying out three different runs at air rates that could be varied, by interchanging calibrated rotameters, over the range from 0.07 to 105 kg/h (1.9 to 2,900 std. ft^3/h). Each column was a section of 20-cm-dia. glass pipe with a conical entry. House air passed through a pressure reducer and through an oil and moisture trap, then into a manifold that conducted it to any or all of the three beds. Rotameter-discharge pressures were indicated by gages at their outlets. To distribute the air evenly beneath each bed, the conical section was filled with 1.9-cm alumina grinding balls to a depth of 15 cm. The test beds were contained in sheet-metal baskets with bottoms made of braced, 10-mesh screen. These were either lowered into the glass pipes after being filled, or filled in place. A thin layer of soft polyurethane foam sealed the narrow radial gap between glass and sheet metal.

The naphthalene used was No. 1-2718 reagent grade furnished by the J. T. Baker Chemical Co. No effort was made to purify this further. This material meets the description of that used by Gil'denblat et al. (1960), whose vapor-pressure data were relied upon in our work. We also used the improved equation fitted to their data by Fowler et al. (1968).

To make a run, several marked naphthalene particles were measured with a micrometer caliper and weighed to the nearest 0.1 mg. Inert material was placed in the bed to a little less than the desired depth, then the naphthalene particles were placed in the bed, well separated from each other and at least two inert-particle diameters from the basket wall. The active particles were then covered with a shallow layer of inert material and the basket with its foam wrapper was slid into the glass pipe. The air rate was adjusted to approximate the desired rotameter reading. The time was noted, and the readings of the rotameter and its outlet pressure gage were recorded as was the barometer reading. Pressure drop through the bed, measured in several high-rate runs, was never more than 25 Pa (0.1 in. of water) and was neglected.

Temperature was measured just above the bed and assumed to be the same within it. After a period of 1 to 5 h, depending on the air rate, the valves were closed, the time noted, the bed was unpacked, and the naphthalene particles were carefully removed, remeasured, and reweighed. The means of the six before and after measurements was used to compute each particle's surface area during the run.

In many of the earlier runs, from three to five spheres were buried in each bed. In the last set of runs, made with rectapipeds, 6, 8 or 14 pieces were typically embedded, two in each different orientation of the three geometries. Figure 2 contains drawings, both isometric and standard projections, of each type, along their nominal dimensions. From these drawings it is clear that while the A lozenges had three possible orientations of a face perpendicular to the bed axis, the others had only two. Note that the second-largest principal dimensions (nominal face diagonals) of the three types are 1.044 cm for A, 2.062 cm for B, and 0.707 cm for C. For each embedded active particle, a set of test data was obtained. In the four families of runs, 349 such particle sets were obtained and have contributed to this report.

The first two stages, using beds of active and inert spheres, were all run in shallow beds, some of which were less than 20 cm in diameter (a filler ring was used) because there were too few balls available in some sizes. Figure 3 shows the placement of three 1.25-cm and two 2.5-cm naphthalene spheres in such a bed. Later, because of reports of entrance effects in ordinary packed beds, we became concerned that these first beds may have been too shallow. After making some check runs in these same shallow beds, we made new runs at the same conditions with beds that were three times as deep. The effect was to position the bed shown in Figure 3 above twice its depth of inert balls.

In Stages 3 and 4, three different shale beds were used. The first consisted of crushed-shale particles passing a standard $^3/_4$-in. (19-mm) screen and retained on a $^3/_8$-in. (9.5-mm) screen, with screen openings of 1.91 and 0.95 cm, and for which the average size was taken as 1.35 cm. The second was the fraction passing the $^3/_8$-in. screen and retained on a 4-mesh screen, with an opening of 0.48 cm, for which the average size was taken as 0.68 cm. The third bed consisted of shale passing a 1-in. screen and retained on a 6-mesh screen (2.54 and 0.336 cm). Several screen analyses of our "masterbatch" crushed shale in this broader size range had determined that the mean particle size, inversely related to the specific surface, equaled 0.98 cm. This mean size is defined by the equation:

$$D_p = 1/\Sigma\left(\frac{m_i}{D_i}\right) \qquad (2)$$

in which m_i is the fraction of the total mass of a screened sample passing the (i-1)st screen and retained on the ith screen (the numbers increasing from the screen with the largest opening to the screens beneath); and D_i is a representative dimension for the material on the ith screen, usually taken as $(O_i \times O_{i-1})^{0.5}$, where O is the screen opening.

The factors studied in this work were of three kinds: those we could closely control, those over which we had partial control, and those we could not control. In the first group

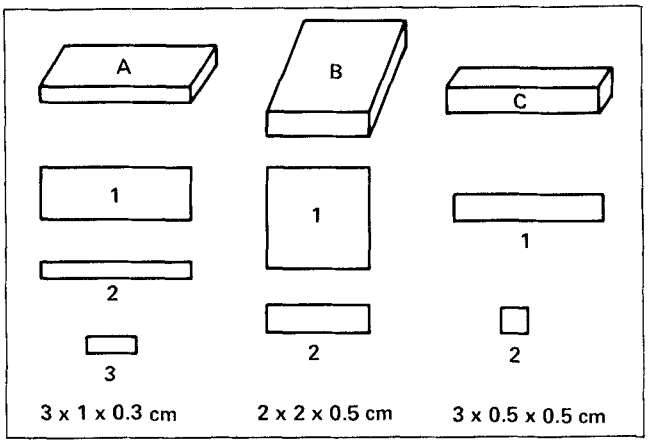

Figure 2. Geometry of rectapiped lozenges with nominal dimensions.

were: (1) the air rate, 0.07 to 106 kg/h; (2) the size and shape of the active particle, spherical from 1.25 to 5 cm, or one of three rectapipeds; (3) mean size of inert balls, 0.3 to 2.54 cm; and (4) size distribution of inert balls, uniform to 10:1 lognormal. In the second group were: (5) shape and size of shale particles; we could control the *mean* size of 0.68 or 1.35 cm in narrow sieve fractions; (6) distribution of shale size, nar-

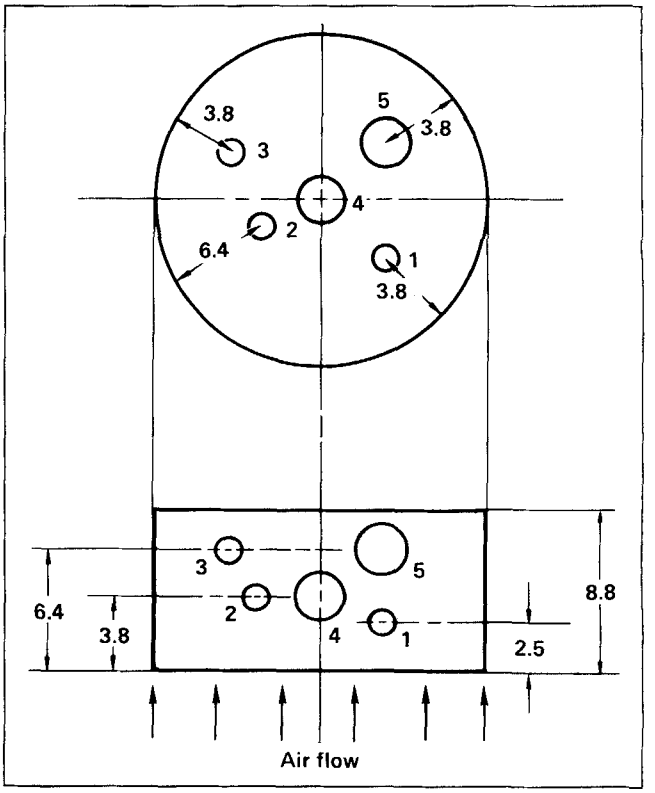

Figure 3. Two views of lognormal ball bed showing placement of 1.27- and 2.54-cm active spheres within bed.

All dimensions are cm.

row or broad; and (7) local void fraction; we had mean void fractions ranging from 0.22 to 0.50. In the third group were air temperature, humidity, and barometric pressure. The latter two varied only slightly. Temperature, which strongly affects the vapor pressure of naphthalene and, through that, the concentration difference from the naphthalene surface to the air stream, ranged from 20 to 29°C over the whole work, but rarely varied more than 2°C during a run. Air properties of interest—viscosity, density, and diffusivity—were only slightly affected. The range of Schmidt numbers in this study was small, about 10%.

Air rate, because of the very wide range achievable, was the dominant factor in this study.

In one set of early runs, the size distribution of the bed, including both the active spheres and inert balls, was designed to simulate that of the distribution for mine-run shale as reported by Matzick et al. (1960). The distribution of diameters in this bed is tabulated below.

Ball size, cm	5.08	2.54	1.90	1.27	0.95	0.64	0.40
Mass %	28	8	8	10	10	11	25

Figure 4 is a plot, on logarithmic-probability coordinates, of the cumulative size distribution which, because of its discreteness, resembles a stairway. This special graph paper is designed so that, if the logarithm of the measured quantity has a normal distribution, its ogive, or cumulative probability plot, will be linear. In plotting size distributions obtained by sieve analyses, the cumulative *mass* fraction (or percent) replaces the classical cumulative numerical frequency on the ordinate scale. The dashed curve in Figure 4 is the mean distribution for mine-run shale as reported by Matzick et al. (1960). Although the median size for our test bed is only one-tenth that of mine-run shale, the plot slopes, and therefore the logarithmic standard deviations of the two distributions are comparable.

We define the mass-transfer coefficient (in dilute binary systems) by the equation

$$\dot{m} = kA\Delta C \cdot 10^{-6} \tag{3}$$

in which $\dot{m}$ = rate of material loss from the active particle, calculated from mass loss and elapsed time, mol/h; A = mean measured area of the surface from which the loss occurs, cm^2; ΔC = the difference between the naphthalene concentrations at the particle surface and in the main air stream passing around the particle, mol/m^3; and k = the mass-transfer coefficient, cm/h. This mass-transfer coefficient differs from that used for typical packed beds in which *all* particles are actively engaged. In such beds, bed volume is easily measured, whereas transfer surface may be uncertain, so the coefficient is based on bed volume.

The naphthalene concentration at the particle surface was taken to be the vapor pressure of naphthalene at the prevailing air temperature, converted to mol/m^3. Naphthalene concentration in the air passing by the particles was not measurable at the particle locales. For each run, the average concentration in exit air was taken as the quotient of the mass evaporated and the mass of air passed through during the run. Even at the lowest air flows, these numbers were so minute

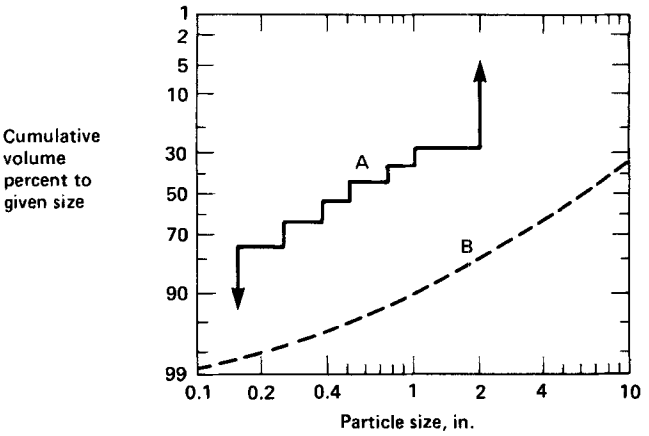

Figure 4. Cumulative size distributions of: (A) lognormal bed of spheres and balls; (B) average for mine-run shale (Matzick et al., 1960).

SI conversion: mm = in. × 25.4.

—never above 0.00006 mol/m^3 and in most runs less than a tenth of that number—that they were negligible, so ΔC was taken to be equal to the concentration at the active particle surface. Areas diminished negligibly in a single run, but particles that were reused were always remeasured before and after being reimplanted in a bed, even though they were stored in tightly closed containers between runs.

Results and Discussion

Active spheres among inert balls

Many ways of presenting mass-transfer data have appeared in the literature, most of them involving dimensionless groups such as the Nusselt, Grashof, Peclet, Stanton, Reynolds, and Schmidt numbers. The Reynolds number, defined below, is the same for both heat transfer and dilute binary mass transfer. The others have analogous, but not identical structures in the two transport modes. These relationships, and the interrelationships among the various groups, are concisely catalogued in Table 21.2-1 of Bird et al. (1960). The Reynolds number is given by

$$Re = \frac{DV\rho}{\mu} = \frac{DG}{\mu} \tag{4}$$

where D = a characteristic size in the flowing stream; V = a characteristic velocity; $G = V\rho$ = mass velocity; ρ = fluid density; and μ = fluid viscosity. For single spheres in a stream, and for packed beds of uniform spheres, D = the sphere diameter. For single *non*spherical particles in a stream, D has frequently been taken as the smallest dimension perpendicular to the overall flow direction. In packed beds of mixed-size spheres, the characteristic diameter has been taken as 6/(specific surface), with specific surface equal to the total surface area of the spheres divided by their total volume (= diameter for spheres of one size).

For beds of particles whose geometry is clean and simple, the same definition has been used and is apparently due to

Ergun (1952), who suggested that a specific surface was the most relevant property of packed beds for fluid drag. He also recommended the same definition for D_p, that is, 6/(specific surface), for beds of irregular particles and mixed sizes, such as we have with crushed oil shale. Other researchers have applied an inversely related shape factor, the particle sphericity, which is unity for a sphere but smaller for all other shapes.

With irregular particles, the total particle surface and volume are not calculable from measured principal dimensions. However, by coating 100 shale pebbles in each of two size ranges with poly(p-xylylene), Carley (1980) was able to measure their surfaces. Volumes were determined by liquid displacement. He then related the specific surface to the measured second-largest principal dimension, the dimension that is presumed to control screen passing. He found, for crushed oil shale, that that dimension—the "particle size"—averaged about 13/(specific surface), or about twice the value for spheres.

For the rectangular lozenges (Figure 2), the second-largest principal (nominal) dimension = $9.7/(A/V)$, $12.4/(A/V)$, and $6.1/(A/V)$ for the A, B and C lozenges, respectively. In a part of the correlation work where we let the active-particle size be inversely proportional to the specific surface, we used the geometric mean of 9.7, 12.4, and 6.1, or 9.0, to represent the rectapipeds.

Another choice to make is the characteristic velocity, V. For single particles in streams, V has usually been taken to be the main stream velocity, well away from the particle (V_∞). For packed beds, some investigators have used the superficial velocity, that is, the volume flow rate divided by the whole cross section of the bed. Our V is this one. Other investigators, for example, Whitaker (1972), have felt that a more meaningful velocity is the flow rate divided by the average open cross section of the bed, that is, superficial velocity divided by void fraction.

Finally, we were working with packed beds in a different way than did our predecessors. Whereas, in most earlier work, *all* the particles in the beds were engaged in whatever transport was occurring, in our beds most of the particles were inert and the active particles were located so that they would not interact. In that respect, they somewhat resembled lone particles immersed in a stream. So there was a real question as to whether the size of the active particle would govern the transfer rate or that of the surrounding inert particles, or both.

We began Stage 1 with beds of spheres in which both the active and inactive particles were of the same size, then investigated various size contrasts to try to answer this question.

The main focus of this work was to develop information on heat convection between air and broken shale. We therefore correlated our measurements in terms of the Chilton-Colburn j_D-factor for mass transfer because that group is equal to the analogous one for heat transfer, both being the same function of Reynolds number.

$$j_D = \frac{k}{V}\left(\frac{\mu}{\rho D_{NA}}\right)^{2/3} = j_H = \frac{h}{C_p V \rho}\left(\frac{C_p \mu}{K}\right)^{2/3} = f(N_{Re}) \quad (5)$$

where k = mass-transfer coefficient; V = characteristic velocity; μ = gas viscosity; ρ = gas density; D_{NA} = diffusivity of naphthalene in air; C_p = gas heat capacity at constant pressure; h = heat-transfer coefficient; and K = gas thermal conductivity. The groups in parentheses are the Schmidt and Prandtl numbers. Under our experimental conditions, the concentrations of naphthalene were so low that they did not influence air-stream properties. The only factor influencing Schmidt number was temperature. We let V = superficial velocity and our Reynolds number was defined as $D_pG/[1.5\mu(1-\epsilon)]$, where ϵ = the average void fraction of the bed. This is identical with Ergun's (1952) except for the tortuosity factor, 1.5, included in the Reynolds number by some workers, not by others. Also, as will be shown, we found that our data correlated more closely when the j_D factor was multiplied by ϵ.

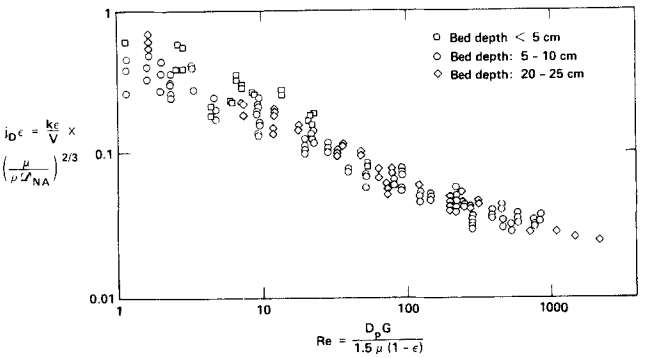

Figure 5. Results obtained in beds of different depth.

Effects of bed depth. As was mentioned earlier, we feared that our early runs might have been biased because the beds were too shallow. Some of them had been made in beds barely 5 cm deep. Most of those run conditions were later repeated using much deeper beds. Figure 5 shows the results for all these runs, all made with naphthalene spheres in beds of inert balls, 159 points in all. The three plotting codes correspond to the different bed-depth ranges. These points appear to be a homogeneous set showing no dependence of $j_D\epsilon$ on bed depth. In this plot, groups of three to five points of the same symbol at one, or closely adjacent Reynolds numbers represent measurements made on replicate spheres in a single bed. The slight differences among Reynolds numbers are due to small differences in sphere sizes. (Spheres were reused in subsequent runs, so became a little smaller as time went on. Interestingly, both they and the rectapipeds retained their true shapes during runs.) Typical mass losses from 1.27-cm spheres were on the order of 10 to 50 mg, somewhat less at the lowest flow rates. The vertical scatter within these point clusters is representative of the variation in transfer rates because of local variations in bed geometry and air velocity. These appear, on this logarithmic scale, to be a little larger at Reynolds numbers below 3. In that region, air velocities are so low that the thickness of the "stagnant film" controlling the rate of convective mass transfer is of the order of the interstitial distances. Below $Re < 3$, diffusion is superseding convective transport as the rate-controlling mechanism.

Nevertheless, the logarithmic differences between duplicate particles are homogeneous enough so that they may be pooled, along with the within-run, particle-size, particle-

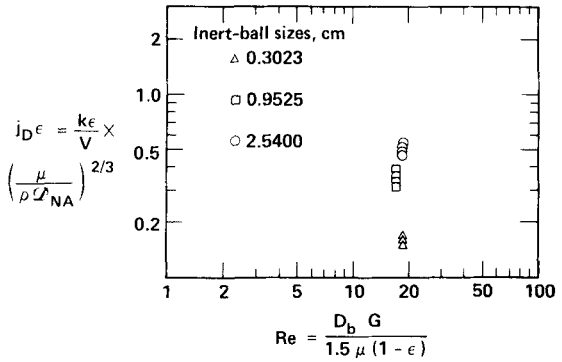

Figure 6. Reynolds number based on inert-ball sizes vs. Chilton-Colburn group. It shows no correlation, but substantial among-groups spread.

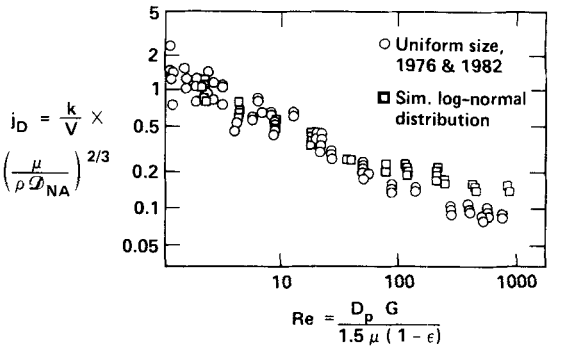

Figure 8. With ordinate j_D and above $N_{Re} = 20$, points for lognormal ball bed diverge upward from those for monodisperse beds.

shape, particle-orientation degrees of freedom to calculate the mean within-cluster variance of the logarithm of the mass-transfer coefficient, and its square root, the standard deviation. With 194 degrees of freedom, that value is 0.0439 ($\log_{10} k$) unit, equivalent to a coefficient of variation in k of 10.6%.

Which particle size controls? To answer this question, we made a suite of three runs, each with five 12.7-cm naphthalene spheres in beds containing inert balls in three single-size levels: 3-mm glass beads, 9.5-mm ball bearings, and 25.4-mm ball bearings, a size spread of 8-fold. Figure 6 shows the results of these runs with the Reynolds numbers computed from the *inert*-ball diameters. The gas rates were chosen in inverse ratio to the sizes, making all these Reynolds numbers closely equal. The j_D values have stacked up, showing highly significant run-to-run differences, and no correlation with these Reynolds numbers. In Figure 7, we see the same data, but with Reynolds number based on the active-sphere size, 1.27 cm; the familiar downtrend is plain. Inverse experiments —runs made with variously sized *active* spheres at constant inert-ball diameter and gas rate—supported the same conclusion: the size of the active particle appears to be the more relevant one for mass transfer. We'll revisit this question later when we discuss the multiple-regression work.

Lognormal size distribution. Earlier we mentioned a large suite of runs in which the size distribution of the bed, including a few 1.27-cm and 2.5-cm active spheres, was approximately lognormal (Figure 4). The results of these runs, along with those in which the beds had uniform sizes, are shown in Figure 8. In this plot, the ordinate is just the j_D-factor. In the region of Reynolds numbers above 10, there is a gradual transition from laminar to turbulent flow (Bird et al., 1960; Ergun, 1952), and flow is mostly turbulent for Reynolds numbers above 100. In that region there is a clear divergence of the two data sets that we believe is attributable mostly to the denser packing and consequent lower void fractions achieved with the lognormal distribution. When these same data are replotted, but with the product of the j-factor and void fraction as the ordinate, the two sets merge into one that is more homogeneous, as Figure 9 shows. The homogeneity at Reynolds numbers above 10, the region of greatest interest for oil-shale retorting, is gained at some sacrifice in the low-N_{Re} region, but with an overall improvement. For this reason, we did our curve-fitting calculations with $j_D\epsilon$ as the dependent variable.

The solid (lower) curve of Figure 10, also shown in Figure 14, summarizes the results of measurements on spheres in beds of balls. It has the equation

$$\log(j_D\epsilon) = -0.2935 - 0.5363 \log N_{Re} + 0.0359 \log^2 N_{Re}. \quad (6)$$

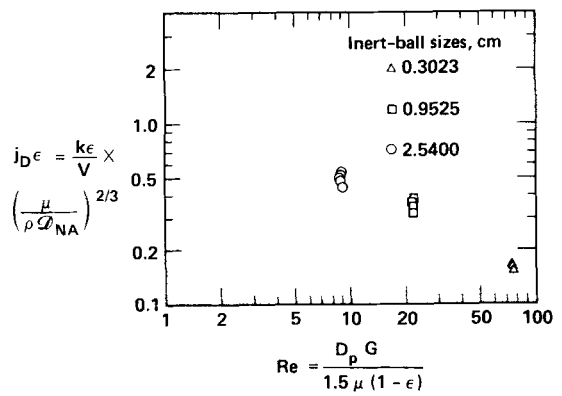

Figure 7. Data of Figure 6 replotted with N_{Re} based on active-sphere size.

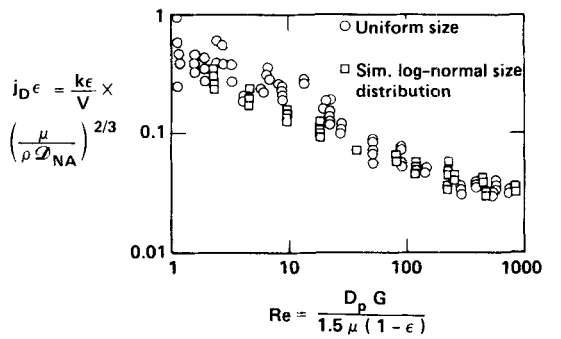

Figure 9. Data of Figure 8 replotted with ordinate $j_D\epsilon$ are more homogeneous at Reynolds numbers above 20.

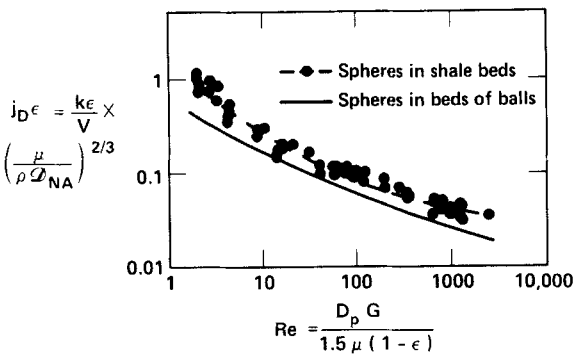

Figure 10. When immersed in beds of crushed shale, active spheres experience higher transfer rates than in ball beds.

Our equations are not directly comparable with those fitted to Whitaker's (1972) Figure 6 because of differences in definitions of the ordinates and abscissas. Our Reynolds numbers are smaller than Whitaker's by the factor of the tortuosity, 1.5. His Nusselt number was defined as $(hD_p/k)/[\epsilon/(1-\epsilon)]$, and so contains $(1-\epsilon)$ in its denominator, not present in ours. Of course, the data he correlated were heat-transfer measurements from five sources, while ours are mass-transfer measurements; but that does not bar comparison, as Eq. 5 guarantees. By the following procedure, we could make a limited comparison. First, taking air at 1 atm (101.3 kPa) and 295 K, and using handbook properties, we chose a D_p value in the range of both groups of data, 1.525 cm, and a typical void fraction, 0.5. For five selected Reynolds numbers (ours), we calculated from Eq. 6 the ordinate $j_D\epsilon = j_H\epsilon = (h\epsilon/C_pG)\cdot N_{Pr}^{2/3}$ and solved this for h. The nearly straight curve of Whitaker's Figure 6 may be replaced with negligible error by the original simpler equation:

$$N_{Nu}N_{Pr}^{-1/3} = 0.60\,N_{ReW}^{-0.60} \qquad (1)$$

where $N_{Nu} = (hD_p/k)/[\epsilon/(1-\epsilon)]$ and $N_{ReW} = D_pG/[\mu(1-\epsilon)] = 1.5\times$ our N_{Re}. From the adjusted Reynolds numbers we calculated $N_{Nu}N_{Pr}^{-1/3}$ from Eq. 1 and solved the expression for h, as before. The results are listed below; the h values are listed below.

N_{Re} (ours)	10	40	140	530	2,000
h (Eq. 6)	0.643	1.390	2.941	6.88	16.98
h_W (Eq. 1)	0.812	1.865	3.954	8.79	19.50

Since most of the data sets included by Whitaker (1972) were measurements made on beds of monodisperse spheres, one might expect our spheres-in-balls data (Eq. 6) to be fairly comparable to his. The preceding table shows that our coefficients are consistently lower, by about 21%. One explanation is that Whitaker's fitted line was elevated by a large, distinctly higher data set of McConnachie and Thodos (1963) that averaged 50% higher heat-transfer coefficients than other data having equal Reynolds numbers. These data arose from a clever experiment in which spheres were arranged on wire supports so as to form a distended, body-centered-cubic arrangement with an average void fraction of 0.78. No sphere touched any other, so their behavior was much more like that of isolated individuals than of spheres in a packed bed. If this data set is deleted from Whitaker's collection, his curve drops about 15%, bringing his h values into close agreement with our Eq. 6. Dropping the atypical data set also reduces the scatter of points around Whitaker's curve to about the same level as ours.

Part 2: Active particles in crushed shale

Spheres in crushed shale. The next suite of runs was an extensive series made with naphthalene spheres in beds of crushed shale. As mentioned earlier, some of these beds contained pebbles in two narrow-size ranges (openings of passing and retaining screens in 2:1 ratio) while other beds contained broadly distributed −2.5-cm shale. We found no significant differences in mass-transfer coefficients, other factors being equal, among these bed types. The results for all are shown in Figure 10 (points and dashed curve). In the range of N_{Re} from 10 to 1,000 the dashed curve lies about 30% higher than the old, lower curve based on data for spheres in beds of balls. Thus, at equal Reynolds numbers, based on the active-sphere diameter, transfer rates were about 30% higher in shale beds than in ball beds. Apparently the irregular channels, causing greater turbulence, and possibly the closer embrace of the active particles by the crushed shale, reduce the thickness of the stagnant film.

Lozenges in shale. Next, a suite of five runs, including transfer-rate measurements on 70 rectapipeds in beds of crushed shale, was made to determine the influence of shape and orientation of the active particle on the rate of naphthalene evaporation. Nominal particle dimensions are shown in Figure 2. (In calculating the Reynolds number and mass-transfer coefficient, the actual mean dimensions and mean surface area during the run for each particle were used.) When the Reynolds number was based on the traditional smallest dimension perpendicular to the bed axis (net direction of gas flow), we obtained the plot shown in Figure 11. Each run or pair of runs corresponding to the plotting codes contained a pair of each of the three particles in the possible different attitudes, 14 in all. Although this plot shows the same downward trend seen in the preceding ones, there is a

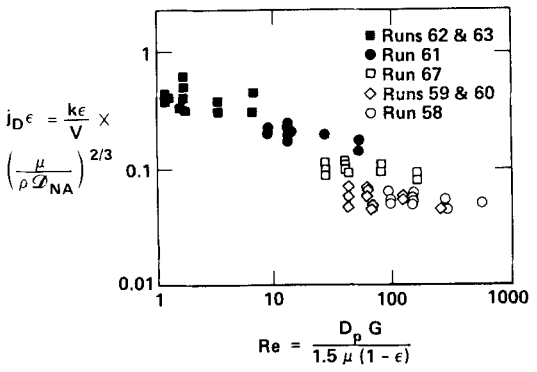

Figure 11. Rectapipeds of all three forms and orientations. They appear to have roughly equal transfer coefficients at given air rates, even though their Reynolds numbers, based on the smallest dimension crosswise to flow, range over nearly an order of magnitude.

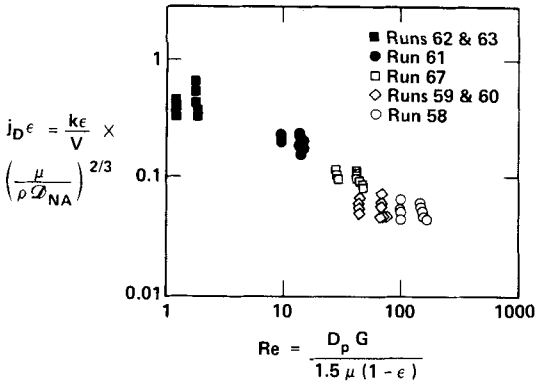

Figure 12. Data of Figure 11, with Reynolds number based on smallest dimension without regard to orientation.

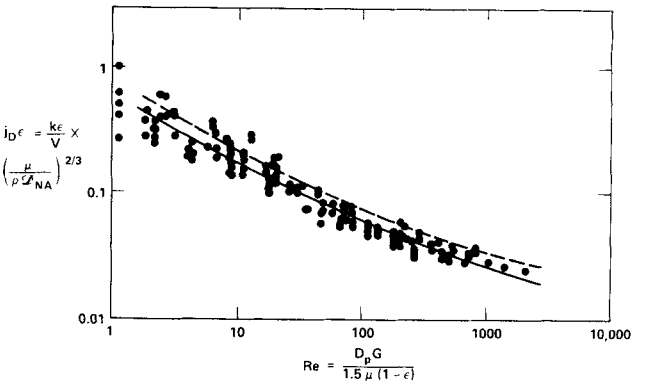

Figure 14. Results for all 349 particle runs.

Points are for spheres in balls, with solid curve (Eq. 6). Dashed curve is least-squares fit to data for spheres and lozenges in crushed shale.

pattern of nearly equal $j_D\epsilon$ values (and k values) for all the particles of each run group. Since the differences in their Reynolds numbers were due only to the difference in their D_p values, this pattern cast doubt on our choice of the characteristic dimension for N_{Re}. When these 70 data pairs were replotted with N_{Re} based on the smallest dimension regardless of orientation, Figure 12 was the result. These grouped a little more tightly, but that choice of dimension was impossible to rationalize.

We decided to return to Ergun's concept, that is, to relate the effective particle size to the specific surface, in this case to let $D_p = 9V/A$, and to make five more runs using size particles in each. Figure 13 is the resulting plot; it looks more consistent than either of the other two. It also shifts most of the points a little to the right with the result that this set is quite compatible with the earlier one (Figure 10) for spheres in shale beds. The final dimensionless-group plot, Figure 14, contains the points and solid curve for spheres in balls, while the dashed curve represents the combined spheres and rectapipeds in crushed oil shale. *The equation for the dashed curve is our recommended equation, of the traditional dimensionless form, for modeling work with oil-shale beds.* It is

$$\log(j_D\epsilon) = -0.0747 - 0.6344\log N_{Re} + 0.0592\log^2 N_{Re}. \quad (7)$$

The standard error of the estimate (with 165 deg of freedom) for the dashed curve is 0.1289 $\log_{10}(j_D\epsilon)$ unit, which corresponds to +35% or −26% of $j_D\epsilon$. The coefficient of determination, R^2, which is interpreted as the fraction of the total variation in $\log(j_D\epsilon)$ that has been accounted for or "explained" by the fitted equation, is 0.89.

Multiple-regression work. Another way to analyze our data is to look upon the mass-transfer coefficient as a purely empirical function of the various experimental factors, choose some reasonable functional form, then evaluate the coefficients of that form by multiple regression. A simple product-of-powers function, not unlike those of the traditional approach, was chosen. Since our air properties are all dependent on temperature, varied only slightly, and are closely correlated, we used air temperature as one of the factors, rather than individual properties. The effect of temperature on naphthalene vapor pressure is the strongest component of this factor's effect. The proposed equation was

$$k = aw_A^b D_p^c \epsilon^d D_b^e t^f \quad (8)$$

which converts logarithmically to

$$\log k = \log a + b\log w_A + c\log D_p + d\log\epsilon + e\log D_b + f\log t \quad (9)$$

where D_b = the specific-surface-averaged mean particle size for the whole bed and t = air temperature, °C. From the loglog plots of the dimensionless groups, in which air rate was the very dominant factor in Reynolds number, it seemed clear from the curvature of most of those plots that the dependence of $\log k$ on $\log w_A$ would *not* be purely linear, so we included an additional term in $\log^2 w_A$. Note that there is no simple inverse transformation of such a term into the power form of Eq. 8. The Minitab program (1983), and its forward-selection procedure, were used in this work.

As in the other format, we found that the data sets for inert-ball beds could be represented by one equation of this form, while those taken in beds of crushed shale required a second equation. The latter one, relevant to oil-shale modeling, is

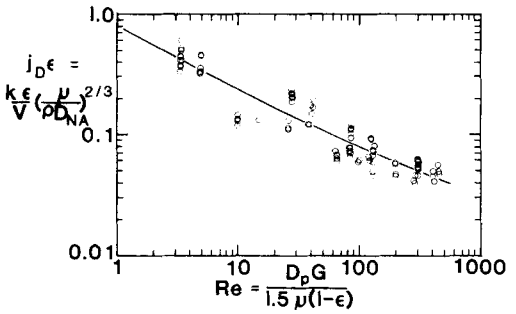

Figure 13. Data of Figure 11, with N_{Re} based on $D_p = 9/(A/v)$.

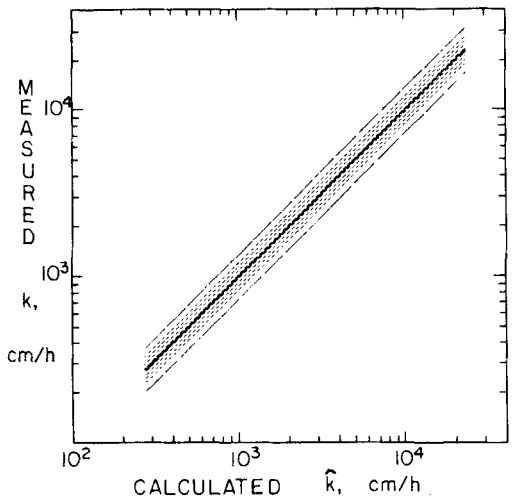

Figure 15. Correlation plot for mass-transfer coefficients with clustering of 349 runs around fitted line; measured $k = \hat{k}$ from regression fit. Only 14 points fell outside the dashed limits.

$$\log(k, \text{cm/h}) = 0.7965 + 0.00994 \log w_A + 0.0702 \log^2 w_A - 0.2112 \log D_p + 0.1728 \log \epsilon - 0.1782 \log D_b + 1.2248 \log t \pm 0.0697 \quad (10)$$

The linear term in $\log w_A$ has a small (but statistically significant) coefficient and could be neglected with minor loss of precision. The curvature is such that it matches the quadratic term very closely. Nevertheless, the curvature *is* very gentle and if the quadratic term is omitted, the linear term becomes strong and does most of the job. The residual standard error of the estimate, however, rises from 0.0697 to $0.0803 \log k$ unit.

The standard error of Eq. 7 has an antilog equal to 1.174, which can be interpreted as a coefficient of variation for k of 17.4 %. Figure 15, a plot of measured k vs. the k-value estimated from either Eq. 10 or its sister equation for beds of balls, shows the 1-standard-error band as the shaded region on both sides of the line $k = \hat{k}$. This plot is a combined one for all the data, 349 particle-runs. Of those, 69% fell within the shaded band, while 96% fell within the wider band defined by the outer, dashed lines. For estimating mass-transfer coefficients in beds of crushed shale, Eq. 10 has error limits about half as wide as those associated with Eq. 7.

There are two cautions: (1) Since gas properties varied only slightly in this work, their role is ill-defined by these equations, in either the traditional or multiple-regression form. The dimensionless groups have theoretical validity based on dimensional analysis, so may be more reliable when dealing with retorting gases at high temperatures. (2) Both equations are subject to extrapolation errors when applied to conditions outside the experimental ranges of their factors. The further you extrapolate, the bigger the possible errors!

Experimental errors. As was noted earlier, the variation among mass-transfer coefficients of nearly identical particles residing in a single bed is about 11% (relative standard deviation). This is far larger than any of the errors ($\leq 1\%$) in our basic measurements, namely, mass evaporated, duration of run, particle dimensions, air temperature, barometric pressure, and rate of air flow. It seems clear that the variations in local bed geometry and air flow, even with uniform spheres, dominate the point-to-point reproducibility.

There is a possible source of bias in our coefficients and Schmidt numbers: the vapor pressure of naphthalene. (We were not equipped to measure this ourselves.) Even traces of volatile impurities can seriously inflate naphthalene vapor pressure. If such impurities were to elevate the vapor pressure above those reported by Gil'denblat et al. (1960), our mass-transfer coefficients would be too high as calculated, in proportion to the error in the vapor pressure.

Another source of possible bias, which affects only our Schmidt numbers, is in the naphthalene diffusivities, due in part to the same basic cause, vapor pressure. In searching the naphthalene literature, we found that all handbook listings of naphthalene diffusivities in air, most of which refer to the International Critical Tables (1929), are traceable to a *single datum* in Table I of a paper by Edward Mack, Jr. (1925). Space does not permit a detailed discussion of Mack's work here, but it is clear that the value of vapor pressure he used, and attributed to earlier work by Barker (1910), was 21% above that now believed to be correct for reagent-grade naphthalene (Gil'denblat et al., 1960; Fowler et al., 1968). We corrected our diffusivities for this error. However, there are at least two other sources of possible error in Mack's measurements that we have not tried to evaluate, one of which would tend to offset the vapor-pressure error. Because of these uncertainties in diffusivity, our Schmidt numbers might be in error by as much as $\pm 20\%$, corresponding to $\pm 13\%$ in the 2/3 power of N_{Sc}. While this does not affect the integrity of the internal contrasts developed in this study, it does affect the comparison of our results with those of other workers using different materials.

Conclusions

In this work, deep and shallow beds gave equal transfer rates from embedded active particles, probably because the entering flow was well distributed.

Mass-transfer coefficients in all the beds varied among identical particles with a relative standard deviation of 11%. This is more than ten times the variation attributable to measurement errors and is believed to be due to local differences in bed geometry and air velocity.

The size of the active particle was more relevant than whole-bed mean size in correlating the Chilton-Colburn mass-transfer factor with Reynolds number. In retort modeling, Reynolds numbers and coefficients of heat and mass transfer should be based on the local sizes rather than the whole-bed average.

The data for spheres and rectapipeds in shale beds form a homogeneous set if the size for the latter is taken as $D_p = 9/(\text{specific surface})$. For shale particles, $D_p = 13/(\text{specific surface})$ is appropriate. Rates for all active particles in shale beds averaged 26% higher than for spheres in beds of inert balls. The dimensionless-group equations gave coefficients of determination (R^2) of 89% with relative standard errors of $+34\%$, -25% of $j_D\epsilon$. Heat-transfer coefficients calculated

from our mass-transfer equation for naphthalene spheres in inert balls were about 6% lower than those obtained from the equation of Whitaker (1972) after removal of an atypical data set from his data body.

Although the only crushed rock worked with was oil shale, we feel that our Eq. 7 will more accurately represent convective transfer in beds of other crushed or otherwise irregular materials than will older correlations based mainly on measurements of transfer in beds of spheres.

Acknowledgments

The work was performed under the auspices of the U.S. Department of Energy by the Lawrence Livermore National Laboratory under contract number W-7405-ENG-48. We are very grateful to the Office of Equal Opportunity, which provided funds for Swecker's participation in this work. We thank T. C. Erven, who cleverly designed, machined, and tested the molds for casting naphthalene particles. Thanks, too, to R. J. Cena, who helped us with computer programming. This report has benefitted greatly from the comments and suggestions of the *Journal's* conscientious reviewers.

Notation

A = area of particle surface
C = vapor concentration in air
C_p = specific heat of gas at constant pressure
D_b = volume-weighted average particle size for bed
D_{NA} = diffusivity of naphthalene in air (= D_{NA} in plots)
D_p = size of active particle = diameter for a sphere, 9/(specific surface) for rectapipeds, 13/(specific surface) for crushed-shape particles
G = mass velocity of air stream = $V \cdot \rho$
h = heat-transfer coefficient at particle surface
j_D = dimensionless Chilton-Colburn mass-transfer factor (Eq. 4)
j_H = dimensionless Chilton-Colburn heat-transfer factor = j_D (Eq. 4)
k = mass-transfer coefficient (Eq. 2)
K = thermal conductivity of gas
$\dot{m}$ = rate of mass loss from active particle
N_{Nu} = Nusselt number, defined by Whitaker (1972) = $(hD_p/K)/[\epsilon/(1-\epsilon)]$
N_{Pr} = Prandtl number = $C_p \mu/K$
N_{Re} = Reynolds number, = $D_pV\rho/[1.5\mu(1-\epsilon)] = D_pG/[1.5\mu(1-\epsilon)]$
N_{ReW} = Whitaker's (1972) Reynolds number = $D_bG/[\mu(1-\epsilon)]$
R^2 = coefficient of determination, the square of the multiple-correlation coefficient
v = volume of active particle
V = superficial air velocity = (volume flow rate)/(bed cross section)

Greek letters

ϵ = average void fraction in bed
μ = viscosity of flowing gas
ρ = density of flowing gas

Literature Cited

Barker, J. T., "Experimentelle Bestimmung und thermodynamische Berechnung der Dampfdrucke von Toluol, Naphthalin und Benzol," *Z. Phys. Chem.*, **71**, 235 (1910).

Bird, R. B., W. E. Stewart, and E. N. Lightfoot, *Transport Phenomena*, Wiley, New York (1960).

Carley, J. F., "Dimensions, Exterior Surfaces, Volumes, Densities and Shape Factors for Particles of Crushed Colorado Oil Shale in Two Narrow Sieve Fractions," *UCRL-84583*, Lawrence Livermore National Laboratory (May, 1980).

Ergun, S., "Fluid Flow through Packed Columns," *Chem. Eng. Progr.*, **48**, 89 (1952).

Fowler, L., W. N. Trump, and C. E. Vogler, "Vapor Pressure of Naphthalene—New Measurements between 40° and 180°C," *J. Chem. Eng. Data*, **13**, 209 (1968).

Gil'denblat, I. A., A. S. Furmanov, and N. M. Zhavoronkov, "Vapor Pressure over Crystalline Naphthalene," *J. Appl. Chem. U.S.S.R.*, **33**, 245 (1960).

International Critical Tables, Vol. V, McGraw-Hill Book Co., p. 63 (1929).

Kunii, D., and O. Levenspiel, *Fluidization Engineering*, Krieger, Huntington, NY, p. 212 (1977).

Kunii, D., and M. Suzuki, "Particle-to-Fluid Heat and Mass Transfer in Packed Beds of Fine Particles," *Int. J. Heat Mass Transf.*, **10**, 845 (1967).

Mack, E., Jr., "Average Cross-Sectional Areas of Molecules by Gaseous Diffusion Methods," *J. Am. Chem. Soc.*, **47**, 2468 (1925) (incorrectly cited in the *International Critical Tables*).

Matzick, A., R. O. Dannenberg, and B. Guthrie, "Experiments in Crushing Green River Oil Shale," *Bur. Mines R.I. 5563* (1960).

McConnachie, J. T. L., and G. Thodos, "Transfer Processes in the Flow of Gases Through Packed and Distended Beds of Spheres," *AIChE J.*, **9**, 60 (1963).

Ryan, T. A., Jr., B. L. Joiner, and B. F. Ryan, Minitab Data Analysis Software, 215 Pond Laboratory, University Park, PA (Jan. 15, 1981).

Whitaker, S., "Forced Convection Heat Transfer Correlations for Flow in Pipes, Past Flat Plates, Single Cylinders, Single Spheres, and for Flow in Packed Beds and Tube Bundles," *AIChE J.*, **18**, 361 (1972).

Manuscript received Sept. 7, 1993, and revision received Apr. 25, 1994.